

---

# REMOTE BIO-SENSING : OPEN SOURCE BENCHMARK FRAMEWORK FOR FAIR EVALUATION OF rPPG \*

---

**Dae-Yeol Kim, Eunsu Goh, KwangKee Lee**  
Innopia Tech  
Gyeonggi-do, Korea  
{wagon0004, dmstn96, kkleee}@innopiatech.com

**JongEui Chae, JongHyeon Mun, Junyeong Na, Chae-bong Sohn**  
Electronics & Communications Engineering, Kwangwoon University  
Seoul, Korea  
{paperc, mjh110311, najubae, cbsohn}@kw.ac.kr

**Do-Yup Kim**  
Department of Information and Communication AI Engineering, Kyungnam University  
Gyeongsangnam-do, Korea  
doyup09@kyungnam.ac.kr

## ABSTRACT

rPPG (Remote photoplethysmography) is a technology that measures and analyzes BVP (Blood Volume Pulse) by using the light absorption characteristics of hemoglobin captured through a camera. Analyzing the measured BVP can derive various physiological signals such as heart rate, stress level, and blood pressure, which can be applied to various applications such as telemedicine, remote patient monitoring, and early prediction of cardiovascular disease. rPPG is rapidly evolving and attracting great attention from both academia and industry by providing great usability and convenience as it can measure biosignals using a camera-equipped device without medical or wearable devices.

Despite extensive efforts and advances in this field, serious challenges remain, including issues related to skin color, camera characteristics, ambient lighting, and other sources of noise and artifacts, which degrade accuracy performance. We argue that fair and evaluable benchmarking is urgently required to overcome these challenges and make meaningful progress from both academic and commercial perspectives. In most existing work, models are trained, tested, and validated only on limited datasets. Even worse, some studies lack available code or reproducibility, making it difficult to fairly evaluate and compare performance. Therefore, the purpose of this study is to provide a benchmarking framework to evaluate various rPPG techniques across a wide range of datasets for fair evaluation and comparison, including both conventional non-deep neural network (non-DNN) and deep neural network (DNN) methods.

GitHub URL: <https://github.com/remotebiosensing/rppg>

**Keywords** rPPG · fair evaluation · remote bio-sensing

## 1 Introduction

Remote photoplethysmography (rPPG), a technology that employs cameras to capture facial images and measure blood volume pulse (BVP) based on optical principles, has gained significant attention in recent years. The analysis of BVP allows rPPG to assess various vital signs, including heart rate (HR), respiration, and blood pressure. The principal

---

\* *Citation*: Authors. Title. Pages.... DOI:000000/11111.

advantage of rPPG lies in its high usability and convenience, which are derived from its minimalistic requirements. It merely necessitates a device equipped with a camera to measure these vital signs.

There has been a surge of interest in rPPG research, resulting in a multitude of published papers and datasets. In response to this trend, the remote physiological signal sensing (REPSS) challenge was conducted at both ICCV [1] and CVPM [2], while the vision for vitals (V4V) challenge occurred at ICCV [3]. More recently, clinical validation and trials for rPPG are being widely undertaken by various institutions [4, 5]. As reported in [6], rPPG demonstrates the capability to accurately measure HR in subjects with cardiovascular disease (CVD).

The exploration of rPPG can be segmented into three principal perspectives: dataset, preprocessing, and model training. From a dataset perspective, rPPG algorithms should account for a variety of characteristics such as subject movement [7–11], region of interest (RoI) [12–20], color space [21], light intensity [22–24], as well as gender and skin color [25, 26]. While diverse datasets are emerging, only a few comprehensively encompass these factors.

With respect to preprocessing, facial cropping methods can be categorized into (i) cropping based on the size of the face (typically a certain multiple of the face’s size), and (ii) tracking facial movement. After facial cropping, different processing methods are applicable, such as (i) continuous method, using the cropped videos as inputs [27–29], (ii) differential normalization method, leveraging frame differences as inputs [30–34], and (iii) spatial-temporal map (STMap) method, converting videos to images, with some deep-learning-based methods, utilizing STMap within deep learning networks [35].

Lastly, from a model training viewpoint, the approaches fall into two categories: (i) non-deep neural network (non-DNN) methods [36–45] and (ii) deep learning methods that utilize various deep learning models.

To address the myriad challenges and issues aforementioned, numerous papers have been published in the rPPG realm. However, a significant fraction of these papers do not openly share their code, thus making a fair evaluation and comparison of the proposed algorithms challenging. The absence of code often compels researchers to reimplement the algorithms from scratch, which leads to potential non-reproducibility due to undisclosed preprocessing and post-processing techniques and specific deep learning model configurations. Moreover, the lack of explicit information regarding train/test/evaluation datasets, such as the time length of the output data used during model evaluation, impedes reproducibility and obstructs fair evaluation and comparisons among different algorithms.

Given these issues, the rPPG research domain tends to be less transparent and more cloistered compared to other research domains. It is highly inefficient for researchers to invest time in reproducing prior works. Hence, this paper aims to provide guidelines for fair evaluation and comparison in rPPG research, and presents an open-source benchmarking framework intended to foster reproducibility and transparency in this field. Through this benchmark project, we aspire to surmount existing limitations, streamline the implementation and evaluation of rPPG algorithms, and enable researchers to have a standardized and comprehensive system for conducting fair and reliable comparisons.

This paper’s primary contributions aim to offer objective and comprehensive information and guideline for rPPG research and development, as follows:

- **rPPG preprocessing techniques:** Given the variance in directory and file structure across public datasets, an efficient interface to access each dataset is essential. Furthermore, the choice of preprocessing methods may vary depending on the deep learning model, such as whether to track faces, crop based on initial face area, crop larger than face size, or crop RoI areas like cheeks and forehead.
- **rPPG dataset lists:** Numerous datasets have been created and made publicly available, but well-organized information about them is lacking. We will provide a comprehensive table detailing each dataset, including supported biometric information, video types (red-green-blue (RGB), near-infrared (NIR)), etc.
- **rPPG models :** Researchers often spend significant time and effort reproducing previous research works. We aim to reduce this time by providing the reference implementation of the key state-of-the-art (SOTA) works in rPPG.
- **rPPG dataset labels:** Typically, datasets provide both photoplethysmography (PPG) and HR labels, but sometimes substantial discrepancies occur between them. Some previous works used HR labels directly from the dataset, while others generated HR labels using methods such as frequency analysis and peak detection.
- **Fair evaluation and comparison:** Some works are not clearly reproduced, and their performance and accuracy cannot be verified. A fairer and more transparent evaluation is achievable by presenting the results obtained through this open-source framework.

## 2 Related Works

In the field of rPPG, there are only a few open-source projects, offering resources for implementing and evaluating rPPG models more efficiently. Such resources enhance the reproducibility and reliability of research findings. Notable examples include:

**rPPG-Toolbox [46]:** The rPPG-Toolbox offers a comprehensive pipeline for rPPG research, development, and evaluation. It incorporates six traditional non-DNN methods, including Green [36], ICA [37], CHROM [39], LGI [43], PBV [40], and POS [41], alongside six deep learning models, including PhysNet [27] and four subsequent Deepphys models [30, 31, 33, 34]. The rPPG-Toolbox distinguishes itself by featuring motion augment training and the latest multi-task learning rPPG model, Bigsmall. It also supports preprocessing for various datasets such as SCAMPS [47], UBFC-rPPG [48], PURE [49], BP4D+ [50], UBFC-phys [51], and MMPD [52].

**iPhys-Toolbox [53]:** Designed for conducting rPPG experiments in the MATLAB environment, iPhys-Toolbox provides a total of six non-DNN methods, including Green [36], ICA [37], CHROM [39], POS [41], and BCG [54] for rPPG analysis and experimentation.

**PPG-I Toolbox [55]:** Launched in 2019 and updated until Oct. 2022, this open-source project focuses on supporting traditional non-DNN methods in rPPG research. Despite the lack of support for deep learning-based methods, it offers capabilities for six traditional non-DNN methods, i.e., Green [36, 56], spatial subspace rotation (SSR) [42], plane-orthogonal-to-skin (POS) [41], local group invariance (LGI) [43], diffusion process (DP) [57, 58], and Riemannian-PPGI (SPH) [55], and five evaluation metrics, i.e., correlation, Bland-Altman, root mean square error (RMSE), mean squared error (MSE), and signal-to-noise ratio (SNR). Note that we also consider these metrics in our work because they are useful to assess various aspects of the performance and accuracy of the rPPG algorithms.

**pyVHR [59]:** It includes its own pipeline for rPPG, offering preprocessing capabilities for 11 open datasets such as PURE [49], LGI-PPGI [43], UBFC-rPPG [48], UBFC-Phys [51], ECG-Fitness [60], MANOB [61], Vicar-PPG-2 [62], V4V [3], VIPL [63], among others. The project provides a variety of methods, including traditional approaches like ICA, PCA, Green, CHROM, POS, SSR, PBV [40], OMIT [64], as well as deep learning methods like HR-CNN [60] and MTTs-CAN [31]. Notably, this project stands out among Python-based open-source projects as it provides an API that offers convenience and ease of use. Additionally, the project provides a visual representation of evaluation metrics, which aids in the analysis and interpretation of results. Overall, this project promotes reproducibility, development, and comparison of rPPG research by providing a comprehensive resource that encompasses various rPPG methods, preprocessing capabilities, open datasets, and evaluation metrics.

**PhysBench [65]:** Physbench offers preprocessing capabilities for 7 rPPG datasets, including RLAP [65], UBFC-rPPG [48], UBFC-PHYS [51], MMPD [52], PURE [49], COHFACE [66], and SCAMPS [47]. In terms of deep learning models, Physbench provides 5 different models: DeepPhys [30], TS-CAN [31], EfficientPhys [33], PhysNet [27], Physformer [28], and Seq-rPPG. Additionally, it offers three non-DNN methods: CHROM [39], ICA [37], and POS [41]. It is noteworthy that the Physformer model is implemented using the PyTorch framework, while the other models are developed using TensorFlow. Apart from the provided models and preprocessing capabilities, Physbench also features a dataset generator that synchronizes input videos with corresponding labels. This allows researchers to create synchronized datasets, which can be useful for training and evaluating rPPG algorithms.

**Terb [67]:** This project is specifically engineered to run rPPG on the edge device Jetson Nano. It supplies two deep learning methods: DeepPhys and PhysNet. These methods are tailored to run rPPG on the Jetson Nano platform.

**bob [68]:** This project offers three non-DNN methods: SSR [42], CHROM [39], and Li's CVPR14 method [69]. These methods are provided to conduct rPPG analysis and experimentation within the project.

## 3 Remote Bio-sensing : Open Source Benchmark Framework for Fair Evaluation of rPPG

We provide an open-source benchmarking framework that ensures the reproducibility of rPPG algorithms and enables fair evaluation. Unlike the existing frameworks that are limited to certain deep learning and traditional models, our benchmarking framework aims to include all SOTA works - all existing and future research works - in the evaluation list. Furthermore, the framework can be extended for researchers to have the freedom to perform preprocessing, add their own deep learning models, and more comprehensive analysis. Offering such flexibility could be a great contribution, not only to a fair evaluation but also to the advancement of rPPG technology itself.

Table 1: rppg open-source project list

Project	[46]	[53]	[55]	[59]	[65]	[67]	[68]	Ours
Open Dataset	Support	O	X	X	O	X	X	O
	# of Dataset	6	-	-	11	7	-	6
	Dataset Analysis	X	-	-	O	X	-	O
non-DNN Method	# of Models	6	6	6	8	3	-	3
DNN Method	Train Support	O	X	X	X	O	O	X
	Evaluation Support	O	X	X	O	O	O	X
	# of Method	5	-	-	2	5	2	-

Table 1 shows an overview of the characteristics of the previously mentioned open-source projects. Our Open-Source framework stands out by offering a dataset analyzer, which is not available in other open-source projects. Additionally, our framework provides a larger variety of methods compared to other existing tools. This allows researchers to explore and evaluate rPPG algorithms using a wider range of techniques, promoting a more comprehensive analysis and comparison of different approaches.

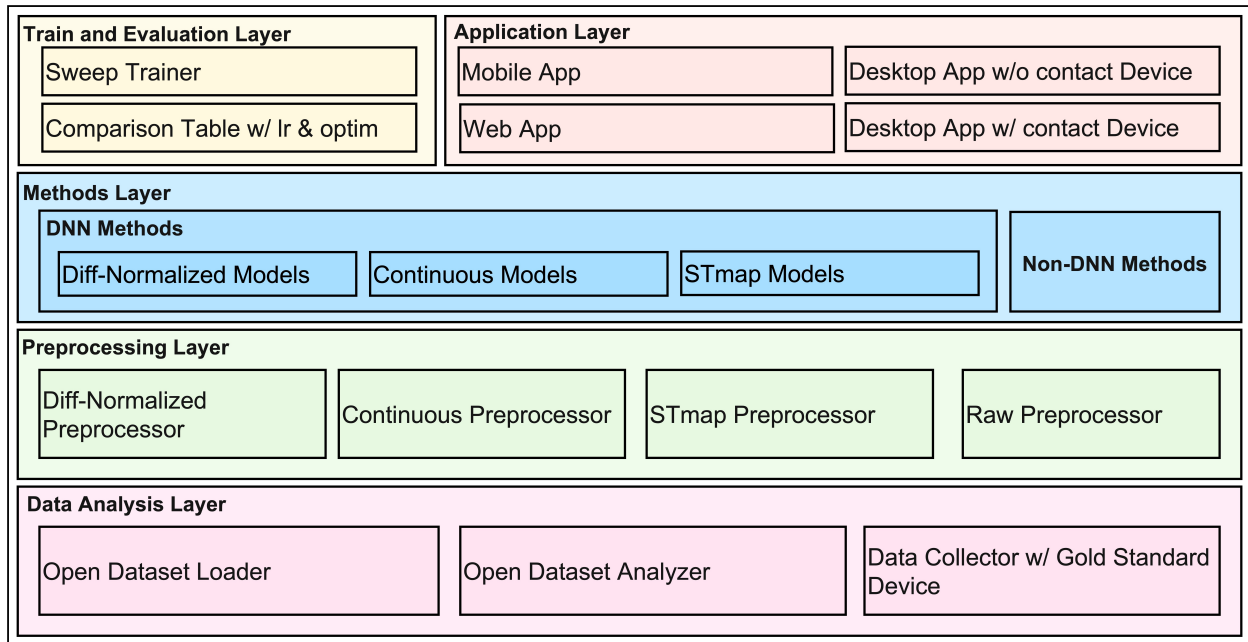


Figure 1: Project Architecture Overview

Figure 1 provides an overview of the proposed open-source project. It consists of four layers that facilitate the implementation and evaluation of rPPG algorithms.

- **Dataset Analysis Layer:** This layer focuses on dataset analysis and provides tools and functions for analyzing the rPPG datasets. It allows researchers to gain insights into the characteristics and properties of the datasets before conducting further preprocessing and modeling.
- **Preprocessing Layer:** This layer is responsible for preprocessing the input data to make it fit and suitable for the following Model Layer. It includes various preprocessing techniques and functions to handle data normalization, filtering, alignment, and other necessary preprocessing steps.
- **Model Layer:** This layer encompasses the implementation of the main processing of the rPPG technology. It includes both DNN and non-DNN methods. Researchers can choose from a wide range of available models based on their specific requirements and preferences.
- **Train and Evaluation Layer:** This layer facilitates the training and evaluation of the DNN models. It provides tools and functions for training the DNN models using the proper datasets and for evaluating the performance of the model using suitable evaluation metrics.

- **Application Layer:** This layer showcases the application of the implemented model by providing demos and examples. It allows researchers to visualize and interpret the results of the rPPG algorithms in practical applications.

Overall, the proposed open-source project offers a comprehensive framework that facilitates dataset analysis, preprocessing, model training and evaluation, and application demonstration, providing researchers with a flexible and integrated platform for their rPPG research and development.

### 3.1 Data Analysis Layer

The Data Analysis Layer provides functionalities related to data collection, retrieval, and analysis. There are over 20 open datasets available, and each dataset has been generated considering different types of information, dimension, artifacts, and noise factors.

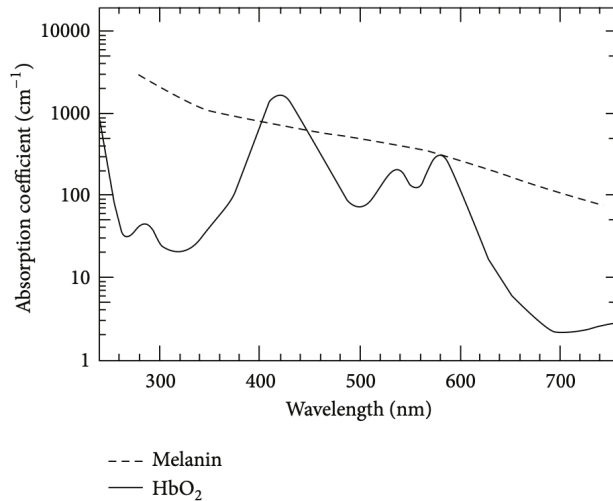
Table 2: OpensDataset List

#	year	name	subject	video	label
1	2011	MAHNOB_HCI [61]	27	RGB	ECG*
2	2012	DEAP [70]	22	RGB	PPG
3	2014	AFRL [71]	25	RGB	PPG
4	2014	PURE [49]	10	RGB	PPG/SPo2*
5	2016	BP4D+ [50]	140	RGB/NIR	PPG/HR*BP*
6	2016	MMSE-HR [72]	40	RGB	HR/BP
7	2017	COHFACE [66]	40	RGB	PPG/HR/RR*
8	2017	BIDMC [73]	-	-	PPG/BP
9	2018	LGGI [43]	25	RGB	-
10	2018	ECG-Fitness [60]	17	RGB	ECG
11	2018	VIPL-HR [63]	107	-	PPG/HR
12	2018	OBF [74]	100	RGB/NIR	PPG/HR
13	2018	MR-NIRP(ind) [75]	8	RGB/NIR	PPG/HR
14	2019	UBFC-rPPG [48]	42	RGB	PPG/HR
15	2020	VicarPPG [62]	10	RGB	PPG/HR/ECG
16	2020	MR-NIRP(DRV) [76]	18	RGB/NIR	PPG/HR
17	2020	mori-ppg [77]	30	RGB	ECG
18	2020	BSIPL-rPPG [78]	37	RGB	PPG
19	2020	EatingSet [62]	20	RGB	PPG/HR
20	2020	StableSet [62]	24	RGB	HR/HRV/ECG
21	2021	UBFC-Phys [51]	56	RGB	PPG/HR/EDA
22	2021	MPSC-rPPG [79]	9	RGB	HR/RR/HRV
23	2021	V4V [3]	140	RGB/NIR	HR/RR/BP
24	2022	MTHS [80]	62	RGB	PPG/RR
25	2022	BAMI-rPPG [81]	14	-	PPG/HR
26	2023	MMPD [52]	33	RGB	PPG
27	2023	Vital Videos [82]	900	-	-

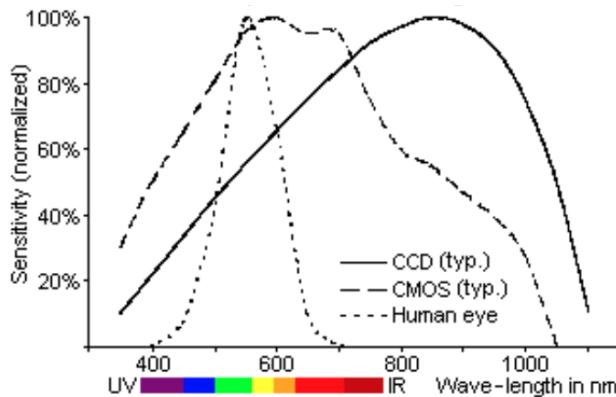
Table 2 presents a list of open datasets. Since the datasets have different structures, it can be time-consuming for new researchers to analyze the data structure. To address this, the Open Dataset Loader assists in easily loading the data based on the analyzed data structure. The Dataset Analyzer offers features such as analyzing the alignment between labels and videos in the open datasets and estimating skin color biases. Additionally, the framework provides features for collecting datasets using a Gold Standard Device in a desktop environment.

#### 3.1.1 Open Dataset Analyzer

rPPG utilizes the optical principle of hemoglobin’s light absorption to observe vascular changes associated with the contraction and relaxation of blood vessels. However, the degree of variation in reflected light due to light absorption is influenced by the thickness of the skin and the content of melanin. Therefore, it is important to consider these factors as well.



(a) Absorption spectra of melanin in skin and hemoglobin(HbO<sub>2</sub>) in blood [83]. Data according to [84]



(b) Camera sensor Spectral Sensitivity [85]

Figure 2: Graph of light absorption of (a)hemoglobin, melanin, and (b)camera sensor according to the wavelength of light

Fig 2 represents the absorption spectra of hemoglobin and melanin at different wavelengths. Hemoglobin exhibits the highest light absorption at 432nm, but camera sensors have lower light sensitivity at this wavelength. Therefore, when measuring rPPG, it is necessary to consider wavelengths with both high light sensitivity and high hemoglobin absorption, which typically fall within the range of 500nm to 600nm. However, within this range, melanin has a higher light absorption rate compared to hemoglobin.



Figure 3: Fitzpatrick scale with Epidermal Melanin [86]

Fig 3 illustrates the melanin content based on the Fitzpatrick scale. As the skin type approaches Type 6, the melanin content increases. This can have an impact on the actual measurement results. However, it is rare for open datasets to provide Fitzpatrick scale as a label, making it challenging to ensure fair evaluations. Therefore, to address this issue, it is necessary to measure skintype. However, measuring the Fitzpatrick scale is a difficult task. In our proposed project, we provide a feature that utilizes [87] to distinguish skin tones, enabling more accurate analysis.

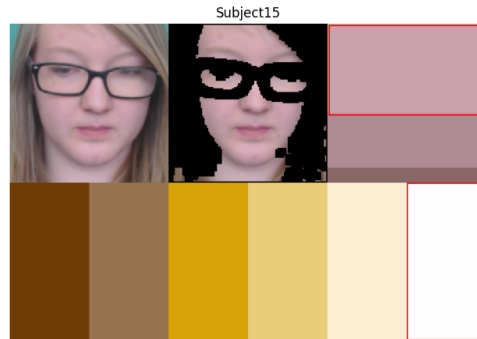


Figure 4: Fitzpatrick scale classification in Open Dataset Analyzer

Figure 4 depicts the results of performing Fitzpatrick scale classification using our Open Dataset Analyzer. By utilizing the predominant color, we were able to distinguish the most similar Fitzpatrick type among the six types. This classification helps in understanding the skin tone variations within the dataset and provides valuable insights for further analysis and evaluation.

rPPG open datasets typically consist of video data and PPG, HR, RR measurements obtained from a pulse oximeter. The oximeter measures PPG by using wavelengths in the IR and RED bands. It compares the emitted light source with the absorbed values to measure the PPG signal and then processes it through a bandpass filter (BPF) and further post-processing to generate vital signs such as HR and RR.

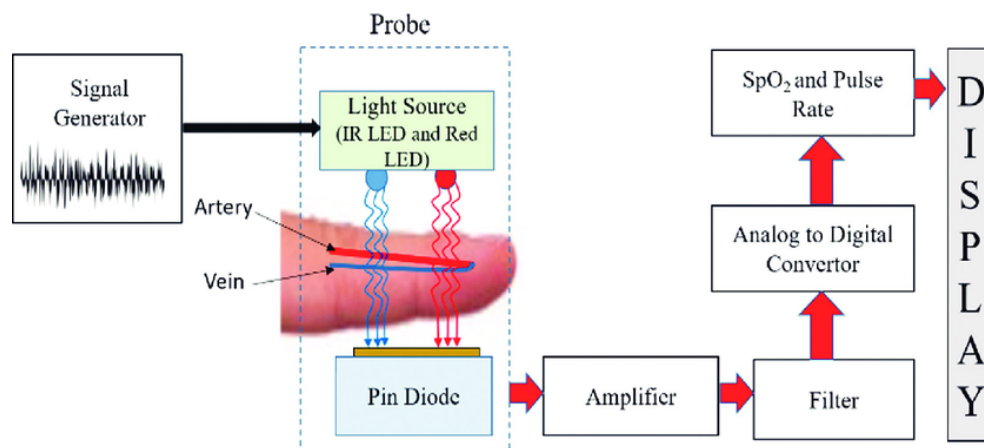


Figure 5: pulse oximeter block diagram [88]

Figure 5 represents a block diagram of a Pulse Oximeter. Generally, when we refer to PPG, it denotes the output of the probe. The internal components of the Oximeter, such as the Filter, ADC, and HR/RR Converter, are responsible for obtaining the HR and respiratory rate (RR) from the PPG signal. However, the settings of the filters and converters (e.g., window size, filter band) can vary across different measurement devices, leading to inconsistencies in the labels provided by open datasets.

To address this issue, when evaluating the performance of algorithms using the PPG labels, it is important to take into consideration the mismatch that can occur between the HR labels and the PPG labels derived from datasets. It is necessary to carefully account for these variations and ensure appropriate alignment between the PPG-based predictions and the corresponding HR labels during evaluation.

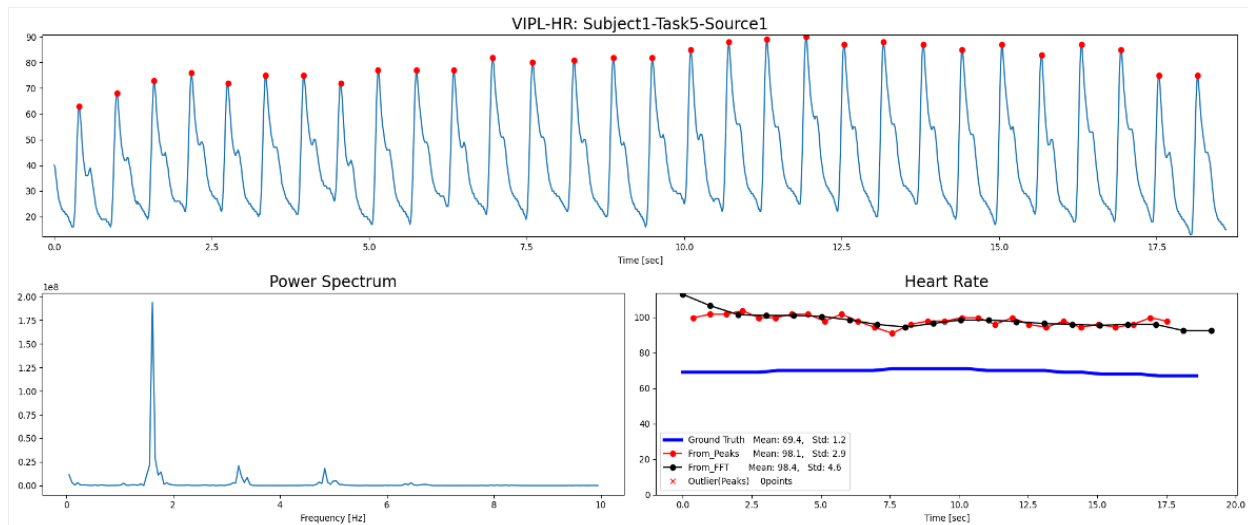


Figure 6: HR estimation at VIPL dataset

Figure 6 shows the results of label evaluation using the Open Dataset Analyzer with the VIPL-HR dataset. Two methods were employed to derive the HR from the given PPG signal: one using peak detection from the PPG signal and the other using frequency analysis. The bottom right graph illustrates the outcomes. The blue line represents the HR provided as the label, the red line corresponds to the HR derived from peak detection, and the black line represents the HR obtained through frequency analysis. It can be observed that there is some discrepancy between the given HR label and the HR derived from PPG. Some research work uses the given HR labels for ground truth and others rely on the derived HR, which causes confusing results and interpretations.

### 3.1.2 Dataset Collector with Golden Standard Device

TBD

## 3.2 Preprocessing Layer

Preprocessing is a time-consuming and challenging task before training DNN-based rPPG algorithms. With the presence of various open datasets that lack a standardized structure and have different formats, we aimed to simplify the preprocessing process by analyzing the storage formats. Our goal was to enable users to preprocess the datasets without the need to understand the underlying structure, and subsequently save the processed data.

To achieve this, we categorized the preprocessing methods into four approaches:

- **DiffNorm:** DiffNorm preprocesses the data by considering the differences between consecutive frames. It takes advantage of the fact that the reflected light from the skin surface changes due to the pulsatile blood flow. By subtracting the current frame from the previous frame, the variations caused by factors such as lighting conditions, camera noise, and static skin properties can be reduced.

$$D(t) = \frac{C'(t) \cdot C(t)}{C(t + \Delta t) - C(t)} \quad (1)$$

Equation represents the preprocessing method of DiffNorm.  $D(t)$  denotes the Diff Normalized data at time  $T$ , and  $C(t)$  denotes the image captured by the camera at time  $t$ . It is based on Shafer's dichromatic reflection model and aims to eliminate the quantization noise from the camera and the component of light reflection. The goal of DiffNorm is to enhance the pulsatile component of the signal while attenuating the non-pulsatile components. By removing the noise and unwanted reflections, it helps to improve the quality and reliability of the rPPG signal for subsequent analysis and modeling.

- **Z-score normalize:** The Z-score normalize method standardizes the data by subtracting the mean and dividing by the standard deviation. It helps in normalizing the data distribution and reducing the influence of outliers.
- **STmap:** STmap refers to representing the video data as a spatial-temporal map, which captures the spatiotemporal information for further analysis. This representation can help in extracting meaningful features and



patterns from the video frames. Figure 7 illustrates the process of generating an STmap from a facial video.

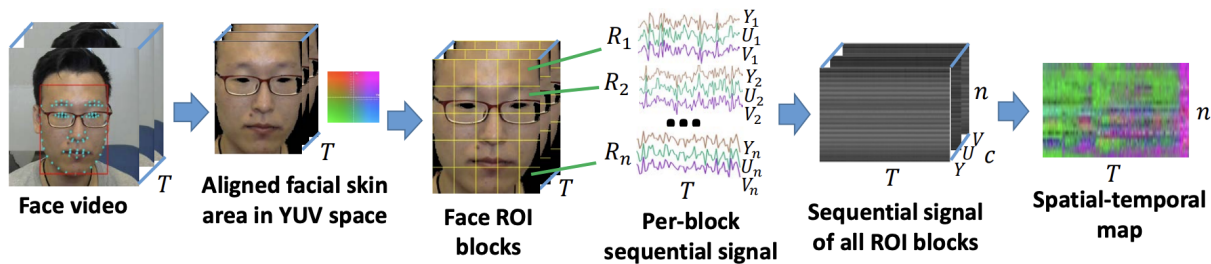


Figure 7: An illustration of spatial-temporal map generation from face video [89]

STmap, or Spatial Temporal map, incorporates spatial transformation information for each frame of video data into a 2D image. This transformation information describes dynamic changes such as object movement, rotation, and scaling.

- **Raw:** The raw method uses the data in its original form without any preprocessing. This approach is useful when the data is already in a suitable format for further processing.

By providing these preprocessing methods, we aimed to alleviate the burden of data preprocessing for users, allowing them to choose and apply the desired preprocessing technique without the need for extensive knowledge of the dataset structure. Additionally, the processed data can be saved for further analysis and training of DNN-based rPPG algorithms.

### 3.3 Model Layer

rPPG is still an active research area using either DNN or non-DNN approaches. Various proposals and efforts are being made in this area. However, some rPPG works lack reproducibility which is not desirable for fair evaluation and further advancement of the technology.

To address this issue, our goal is to tackle the problem by implementing and openly sharing as many rPPG methods as possible. By providing access to the source code of various methods, we aim to promote transparency, reproducibility, and collaboration within the rPPG research community. We believe that by making the implementations available, we can facilitate knowledge sharing, accelerate research progress, and ultimately contribute to the advancement of the rPPG field.

#### 3.3.1 Non-DNN Methods

Table 3 provides summary of non-DNN rPPG measurement methods which are all non-DNN approaches that leverage the domain characteristics of rPPG to compute the signals. These methods utilize different principles and techniques to extract and estimate the rPPG signal from video data without relying on DNN models.

#### 3.3.2 DNN Methods

DNN-based methods in the rPPG field can be categorized based on their input formats, and in our Open-Source Framework, they have been implemented using PyTorch for reproducibility.

Table 4 provides summary of DNN rPPG measurement methods. Deep learning methods are still dependent on the shape of the input, and convergence is determined by the shape of the input.

### 3.4 Train and Evaluation Layer

One of our main objectives is to provide researchers with a convenient research environment. To achieve this, we have incorporated a *fit.yaml* that allows users to easily modify specific configurations, enabling them to customize various aspects of the pipeline, including preprocessing, training, and evaluation. Researchers can make necessary adjustments to suit their experimental setups and research goals by modifying this yaml file. Furthermore, Meta Learning (MAML) [90] option can also be configured with proper settings.

In addition, the benchmark’s hyperparameters are configured in the *model\_preset.yaml*. This allows for better reproducibility by ensuring that the same hyperparameters can be applied consistently across experiments. Additionally, we

Table 3: Summary of Non-DNN rppg measurement methods

input	Method	Representation
Raw [0 ... 255]	GREEN	This method considers the spectral sensitivity of the camera sensor and the light absorption of hemoglobin. It identifies the Green channel as the most suitable for measuring the specular reflection component. It calculates the average Green channel signal and utilizes predominant frequency analysis to estimate the HR.
Raw [0 ... 255]	ICA	Independent Component Analysis (ICA) is employed to separate different signal components mixed within a signal matrix. By applying the JADE algorithm and whitening matrix, the original signals are separated. Empirically, the second separated component is often used as the PPG signal.
Raw [0 ... 255]	PCA	Principal Component Analysis (PCA) is a well-known dimensionality reduction technique. In this context, PCA is applied to analyze the main components of RGB video signals and reconstruct the PPG signal.
Raw [0 ... 255]	CHROM	The CHROM method aims to remove noise caused by light reflection and estimates the PPG signal by filtering out unwanted noise.
Raw [0 ... 255]	PBV	PBV proposes a vector that distinguishes motion noise from pulse-related noise in RGB signals to observe variations in heartbeat.
Raw [0 ... 255]	POS	POS aims to mitigate specular reflection noise. It projects the PPG waveform onto a plane orthogonal to the skin tone, which helps in signal recovery.
Raw [0 ... 255]	SSR	SSR utilizes the absorbance characteristics of hemoglobin. By applying Subspace Rotation and Temporal Rotation, it extends the pulse amplitude and reduces distortion caused by light reflection.
Raw [0 ... 255]	LGI	LGI suggests a robust algorithm using differentiable local transformations to handle various environmental conditions.

Table 4: Summary of DNN rppg measurement methods

Type	input	Method	Representation
Diff Normalized	Z-score Diff Norm	DeepPhys [30]	The first deep learning model based on Shafer's Drm. Measure BVP between two $\Delta T$ using two branch CNN
	Avg(Z-score) Diff Norm	MTTS [31]	Model applying TSM(Temporal Shift Model) to DeepPhys to reduce motion noise Multi-task model aimed at measuring HR and RR.
	Diff Norm(Z-score)	EfficientPhys-C [33]	End-to-End model aimed at simplifying the existing DeepPhys and MTTS preprocessing and operating on mobile devices.
	Z-Score DiffNorm	BigSmall [34]	A Wrapping Temporal Shift Model (WTSM) proposal that produces highly accurate results even with a small number of input frames.
Continuos	Raw [-1 .. 1]	PhysNet [27]	Using negative pearson loss and 3D CNN, rPPG reasoning ability was confirmed.
	Raw [-1 .. 1]	PhysFormer [28]	Propose Curriculum Learning Guided Dynamic Loss and verify rPPG inference performance using Transformer.
	RAW [TBD]	APNET [35]	
STmap	YUV STmap	RhythmNet [89]	Validation of HR Estimation via Video to STmap.

have implemented a sweep functionality to facilitate the reproducibility of experiments. Researchers can refer to the Appendix for more detailed information regarding these configurations and implementation details.

To ensure a fair evaluation of the model, we separated the dataset at the subject level, ensuring that the subjects used for training were not used in the evaluation. Additionally, to analyze the model's prediction accuracy over time duration, we conducted evaluations at intervals of [3s, 5s, 10s, 20s, 30s].

The evaluation methods we employed are as follows:

- Correlation: Correlation coefficient between the predicted values and ground truth values to assess the linear relationship

$$Correlation = \frac{T \sum_1^T \hat{y}y - \sum_1^T \hat{y} \sum_1^T y}{\sqrt{(T \sum_1^T \hat{y}^2 - (\sum_1^T \hat{y})^2)(T \sum_1^T y^2 - (\sum_1^T y)^2)}} \quad (2)$$

- Bland-Altman Analysis: Evaluation of the agreement between the predicted values and ground truth values by examining the mean difference and limits of agreement
- Root Mean Square Error (RMSE): A measure of the overall difference between the predicted values and ground truth values

$$RMSE = \sqrt{\frac{1}{N} \sum (\hat{y} - y)^2} \quad (3)$$

- Mean Absolute Error (MAE): Assessment of the average absolute difference between the predicted values and ground truth values

$$MAE = \frac{1}{N} \sum |\hat{y} - y| \quad (4)$$

- Mean Absolute Percentage Error (MAPE) : The average percentage difference between the predicted values and the ground truth values

$$MAPE = \frac{1}{N} \sum \left| \frac{\hat{y} - y}{y} \right| \quad (5)$$

- Signal-to-Noise Ratio (SNR) [39]: Evaluation of the signal quality of the predicted values compared to the background noise

$$SNR = 10 \log_{10} \left( \frac{\sum_{f=HR_{min}}^{HR_{max}} (U_t(f) \hat{S}(f))^2}{\sum_{f=HR_{min}}^{HR_{max}} (1 - U_t(f)) \hat{S}(f)^2} \right) \quad (6)$$

where  $\hat{S}(f)$  is the spectrum of the pulse signal,  $S, f$  is the frequency in beats per minute, and  $U_t(f)$  is a binary template window as shown in Fig. 3.

By employing these evaluation metrics, we aimed to provide a comprehensive assessment of the model’s performance and ensure a fair and objective evaluation of our trained models.

### 3.5 Application Layer

TBD

## 4 Reproducibility and Benchmark Results

In this chapter, we provide some evidence of the reproducibility of our code and present benchmark results for a fair evaluation of each model. For cross-dataset evaluation, we utilized the UBFC and PURE datasets. Deep learning models such as DeepPhys, TSCAN, EfficientPhys, and Bigsmall were evaluated, while non-DNN methods including CHROM and POS were also assessed.

Among the evaluated models, Bigsmall is a multi-task learning method, but we conducted the evaluation using a single-task learning approach. We assessed the performance of each model using evaluation metrics such as MAE (Mean Absolute Error), RMSE (Root Mean Square Error), MAPE (Mean Absolute Percentage Error), and Pearson-Correlation. These metrics were calculated for time periods of 3, 5, 10, 20, and 30 seconds.

Figure 8 is the inference result according to the length of time. If the time period is increased from 3 seconds to 10 seconds, the evaluation result improves rapidly, and there is no significant change beyond that, and sometimes gets worse.

Figure 9 is the cross-dataset evaluation result. If the dataset has a variety of variables, and the model converges well for the various variables, it can be seen that cross-data set evaluation yields good results. Additional results can be found in the appendix.

With more diverse combinations of building blocks, such as datasets and evaluation metrics, comparison among models will be seen more clearly, and a fair assessment of performance and deeper analysis is possible. Researchers can use these results as a reference for comparing different models and making systematic decisions based on their specific requirements.

## 5 Conclusion

We argue that fair and systematic benchmarking is urgently needed to overcome the challenges in the rPPG technology and make further advancements. To this end, we are proposing a benchmarking framework that enables various rPPG techniques - all existing and future research works - over wide open datasets to be fairly evaluated and compared, including both conventional Non-DNN and DNN methods.

## 6 future work

We intend to keep updating this open-source benchmarking framework that ensures the reproducibility of rPPG algorithms and enables fair evaluation. Important datasets and research works will be continuously added and evaluated

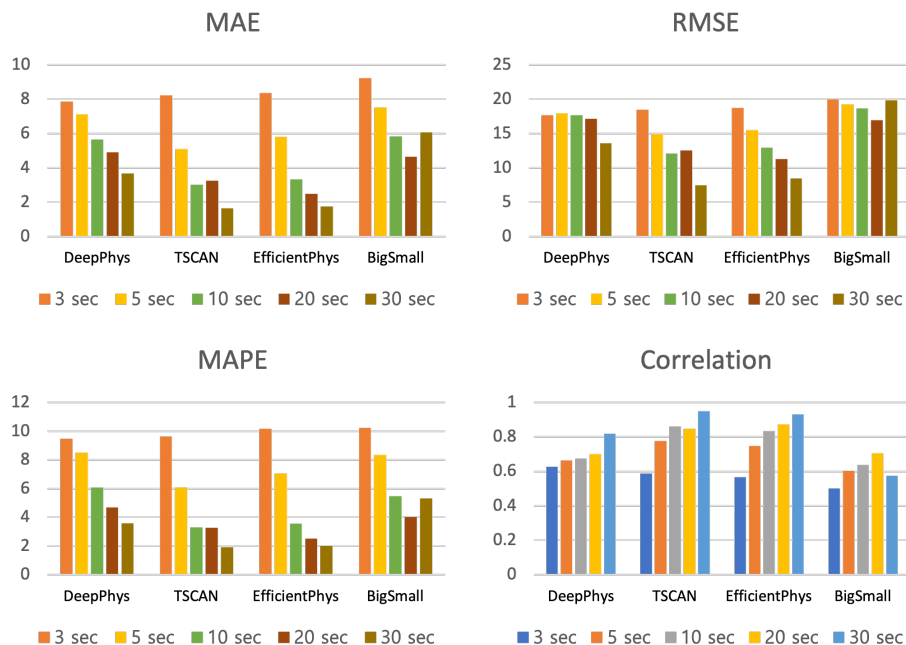


Figure 8: estimate time length evaluation result of UBFC-PURE dataset

accompanied with the comprehensive experiment results and analysis. Furthermore, the framework will be extended for researchers to have the freedom to select preprocessing technology, add their own deep learning models, and conduct a more comprehensive analysis. Offering such flexibility could be a great contribution, not only to a fair evaluation but also to the advancement of rPPG technology itself. We welcome your participation and contribution to this effort.

## Acknowledgments

This was supported in part by.....

## References

- [1] Xiaobai Li, Hu Han, Hao Lu, Xuesong Niu, Zitong Yu, Antitza Dantcheva, Guoying Zhao, and Shiguang Shan. The 1st challenge on remote physiological signal sensing (repps). In *Proceedings of the IEEE/CVF Conference on Computer Vision and Pattern Recognition Workshops*, pages 314–315, 2020.
- [2] *The 2nd Challenge on Remote Physiological Signal Sensing (RePSS)*, 2021.
- [3] *The first vision for vitals (v4v) challenge for non-contact video-based physiological estimation*, 2021.
- [4] Emily Heiden, Tom Jones, Annika Brogaard Maczka, Melissa Kapoor, Milan Chauhan, Laura Wiffen, Helen Barham, Jeremy Holland, Manish Saxena, Simon Wegerif, Thomas Brown, Mitch Lomax, Heather Massey, Shahin Rostami, Laurence Pearce, and Anoop Chauhan. Measurement of vital signs using lifelight remote photoplethysmography: Results of the VISION-D and VISION-V observational studies. *JMIR Form. Res.*, 6(11):e36340, November 2022.
- [5] Edem Allado, Mathias Poussel, Justine Renno, Anthony Moussu, Oriane Hily, Margaux Temperelli, Eliane Albuissou, and Bruno Chenuel. Remote photoplethysmography is an accurate method to remotely measure respiratory rate: A hospital-based trial. *Journal of Clinical Medicine*, 11(13):3647, 2022.
- [6] Theodore Curran, Xin Liu, Daniel McDuff, Shwetak Patel, and Eugene Yang. Camera-based remote photoplethysmography to measure heart rate and blood pressure in ambulatory patients with cardiovascular disease: Preliminary analysis. *Journal of the American College of Cardiology*, 81(8\_Supplement):2301–2301, 2023.
- [7] Yuting Yang, Chenbin Liu, Hui Yu, Dangdang Shao, Francis Tsow, and Nongjian Tao. Motion robust remote photoplethysmography in cielab color space. *Journal of biomedical optics*, 21(11):117001–117001, 2016.

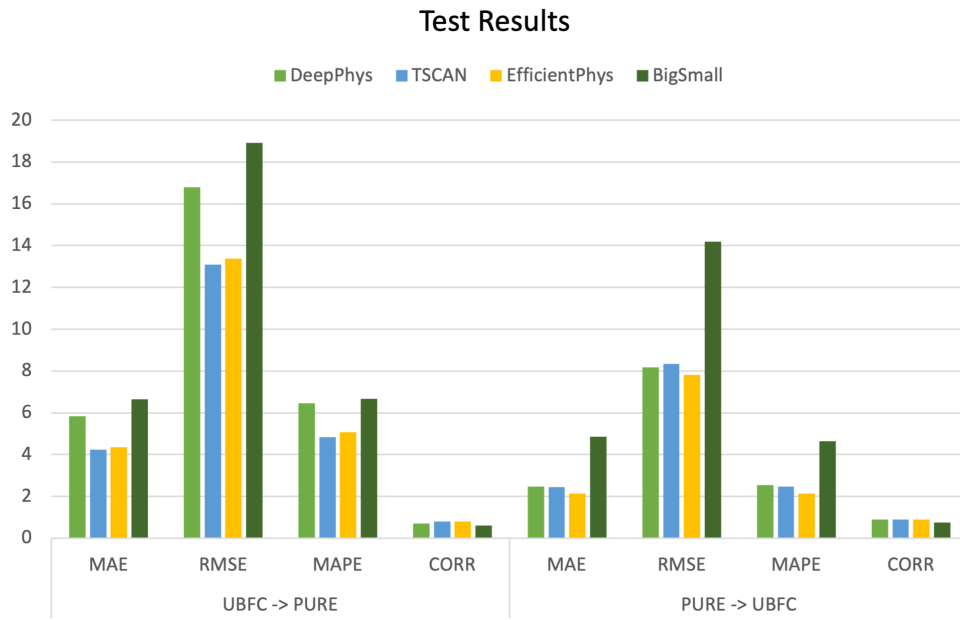


Figure 9: Cross dataset evaluation result of UBFC-PURE, PURE-UBFC dataset (10s)

- [8] Fabian Schrupf, Christoph Mönch, Gerold Bausch, and Mirco Fuchs. Exploiting weak head movements for camera-based respiration detection. In *2019 41st Annual International Conference of the IEEE Engineering in Medicine and Biology Society (EMBC)*, pages 6059–6062. IEEE, 2019.
- [9] Yiming Liu, Binjie Qin, Rong Li, Xintong Li, Anqi Huang, Haifeng Liu, Yisong Lv, and Min Liu. Motion-robust multimodal heart rate estimation using bcg fused remote-ppg with deep facial roi tracker and pose constrained kalman filter. *IEEE Transactions on Instrumentation and Measurement*, 70:1–15, 2021.
- [10] Jianwei Li, Zitong Yu, and Jingang Shi. Learning motion-robust remote photoplethysmography through arbitrary resolution videos. *arXiv preprint arXiv:2211.16922*, 2022.
- [11] Nunzia Molinaro, Federico Zangarelli, Emiliano Schena, Sergio Silvestri, and Carlo Massaroni. Cardiorespiratory parameters monitoring through a single digital camera in real scenarios: Roi tracking and motion influence. *IEEE Sensors Journal*, pages 1–1, 2023.
- [12] Yogesh Deshpande, Surendrabikram Thapa, Abhijit Sarkar, and A Lynn Abbott. Camera-based recovery of cardiovascular signals from unconstrained face videos using an attention network. In *Proceedings of the IEEE/CVF Conference on Computer Vision and Pattern Recognition*, pages 5974–5983, 2023.
- [13] Dae-Yeol Kim, Kwangkee Lee, and Chae-Bong Sohn. Assessment of roi selection for facial video-based rppg. *Sensors*, 21(23):7923, 2021.
- [14] Lai-Man Po, Litong Feng, Yuming Li, Xuyuan Xu, Terence Chun-Ho Cheung, and Kwok-Wai Cheung. Block-based adaptive roi for remote photoplethysmography. *Multimedia Tools and Applications*, 77:6503–6529, 2018.
- [15] Sungjun Kwon, Jeehoon Kim, Dongseok Lee, and Kwangsuk Park. Roi analysis for remote photoplethysmography on facial video. In *2015 37th Annual International Conference of the IEEE Engineering in Medicine and Biology Society (EMBC)*, pages 4938–4941. IEEE, 2015.
- [16] Georg Lempe, Sebastian Zaunseder, Tom Wirthgen, Stephan Zipser, and Hagen Malberg. Roi selection for remote photoplethysmography. In *Bildverarbeitung für die Medizin 2013: Algorithmen-Systeme-Anwendungen. Proceedings des Workshops vom 3. bis 5. März 2013 in Heidelberg*, pages 99–103. Springer, 2013.
- [17] Xuesong Niu, Hu Han, Shiguang Shan, and Xilin Chen. Continuous heart rate measurement from face: A robust rppg approach with distribution learning. In *2017 IEEE International Joint Conference on Biometrics (IJCB)*, pages 642–650. IEEE, 2017.
- [18] Changchen Zhao, Menghao Zhou, Weiran Han, and Yuanjing Feng. Anti-motion remote measurement of heart rate based on region proposal generation and multi-scale roi fusion. *IEEE Transactions on Instrumentation and Measurement*, 71:1–13, 2022.

- [19] Ron Van Luijtelaaar, Wenjin Wang, Sander Stuijk, and Gerard de Haan. Automatic roi detection for camera-based pulse-rate measurement. In *Asian Conference on Computer Vision*, pages 360–374. Springer, 2014.
- [20] Elisa Calvo-Gallego and Gerard de Haan. Automatic roi for remote photoplethysmography using ppg and color features. In *International Conference on Computer Vision Theory and Applications*, volume 2, pages 357–364. SCITEPRESS, 2015.
- [21] Kokila Bharti Jaiswal, Mourya Choubey, Abhinav Mishra, Diksha Singh, and T Meenpal. Color space analysis for improvement in rppg. In *2023 International Conference for Advancement in Technology (ICONAT)*, pages 1–7. IEEE, 2023.
- [22] Ismoil Odinaev, Jing Wei Chin, Kin Ho Luo, Zhang Ke, Richard HY So, and Kwan Long Wong. Optimizing camera exposure control settings for remote vital sign measurements in low-light environments. In *Proceedings of the IEEE/CVF Conference on Computer Vision and Pattern Recognition*, pages 6085–6092, 2023.
- [23] Yu-Chen Lin and Yuan-Hsiang Lin. A study of color illumination effect on the snr of rppg signals. In *2017 39th Annual International Conference of the IEEE Engineering in Medicine and Biology Society (EMBC)*, pages 4301–4304, 2017.
- [24] Lin Xi, Weihai Chen, Changchen Zhao, Xingming Wu, and Jianhua Wang. Image enhancement for remote photoplethysmography in a low-light environment. In *2020 15th IEEE International Conference on Automatic Face and Gesture Recognition (FG 2020)*, pages 1–7, 2020.
- [25] Ewa M Nowara, Daniel McDuff, and Ashok Veeraraghavan. A meta-analysis of the impact of skin tone and gender on non-contact photoplethysmography measurements. In *Proceedings of the IEEE/CVF Conference on Computer Vision and Pattern Recognition Workshops*, pages 284–285, 2020.
- [26] Yunhao Ba, Zhen Wang, Kerim Doruk Karınca, Oyku Deniz Bozkurt, and Achuta Kadambi. Style transfer with bio-realistic appearance manipulation for skin-tone inclusive rppg. In *2022 IEEE International Conference on Computational Photography (ICCP)*, pages 1–12. IEEE, 2022.
- [27] Zitong Yu, Xiaobai Li, and Guoying Zhao. Remote photoplethysmograph signal measurement from facial videos using spatio-temporal networks. *arXiv preprint arXiv:1905.02419*, 2019.
- [28] Zitong Yu, Yuming Shen, Jingang Shi, Hengshuang Zhao, Philip HS Torr, and Guoying Zhao. Physformer: facial video-based physiological measurement with temporal difference transformer. In *Proceedings of the IEEE/CVF Conference on Computer Vision and Pattern Recognition*, pages 4186–4196, 2022.
- [29] Zitong Yu, Yuming Shen, Jingang Shi, Hengshuang Zhao, Yawen Cui, Jiehua Zhang, Philip Torr, and Guoying Zhao. Physformer++: Facial video-based physiological measurement with slowfast temporal difference transformer. *International Journal of Computer Vision*, 131(6):1307–1330, 2023.
- [30] Weixuan Chen and Daniel McDuff. Deepphys: Video-based physiological measurement using convolutional attention networks. *CoRR*, abs/1805.07888, 2018.
- [31] Xin Liu, Josh Fromm, Shwetak Patel, and Daniel McDuff. Multi-task temporal shift attention networks for on-device contactless vitals measurement. *Advances in Neural Information Processing Systems*, 33:19400–19411, 2020.
- [32] Xin Liu, Ziheng Jiang, Josh Fromm, Xuhai Xu, Shwetak Patel, and Daniel McDuff. Metaphys: few-shot adaptation for non-contact physiological measurement. In *Proceedings of the conference on health, inference, and learning*, pages 154–163, 2021.
- [33] Xin Liu, Brian L Hill, Ziheng Jiang, Shwetak Patel, and Daniel McDuff. Efficientphys: Enabling simple, fast and accurate camera-based vitals measurement. *arXiv preprint arXiv:2110.04447*, 2021.
- [34] Girish Narayanswamy, Yujia Liu, Yuzhe Yang, Chengqian Ma, Xin Liu, Daniel McDuff, and Shwetak Patel. Bigsmall: Efficient multi-task learning for disparate spatial and temporal physiological measurements. *arXiv preprint arXiv:2303.11573*, 2023.
- [35] Dae-Yeol Kim, Soo-Young Cho, Kwangkee Lee, and Chae-Bong Sohn. A study of projection-based attentive spatial-temporal map for remote photoplethysmography measurement. *Bioengineering*, 9(11):638, 2022.
- [36] Wim Verkruyse, Lars O Svaasand, and J Stuart Nelson. Remote plethysmographic imaging using ambient light. *Opt. Express*, 16(26):21434–21445, December 2008.
- [37] Ming-Zher Poh, Daniel J McDuff, and Rosalind W Picard. Non-contact, automated cardiac pulse measurements using video imaging and blind source separation. *Opt. Express*, 18(10):10762–10774, May 2010.
- [38] Magdalena Lewandowska, Jacek Ruminski, Tomasz Kocejko, and Jędrzej Nowak. Measuring pulse rate with a webcam - a non-contact method for evaluating cardiac activity. pages 405–410, 01 2011.

- [39] Gerard de Haan and Vincent Jeanne. Robust pulse rate from chrominance-based rppg. *IEEE Transactions on Biomedical Engineering*, 60(10):2878–2886, 2013.
- [40] G de Haan and A van Leest. Improved motion robustness of remote-PPG by using the blood volume pulse signature. *Physiol. Meas.*, 35(9):1913–1926, August 2014.
- [41] Wenjin Wang, Albertus C. den Brinker, Sander Stuijk, and Gerard de Haan. Algorithmic principles of remote ppg. *IEEE Transactions on Biomedical Engineering*, 64(7):1479–1491, 2017.
- [42] Wenjin Wang, Sander Stuijk, and Gerard de Haan. A novel algorithm for remote photoplethysmography: Spatial subspace rotation. *IEEE Transactions on Biomedical Engineering*, 63(9):1974–1984, 2016.
- [43] Christian S. Pilz, Sebastian Zaunseder, Jarek Krajewski, and Vladimir Blazek. Local group invariance for heart rate estimation from face videos in the wild. In *2018 IEEE/CVF Conference on Computer Vision and Pattern Recognition Workshops (CVPRW)*, pages 1335–13358, 2018.
- [44] Rencheng Song, Jiji Li, Minda Wang, Juan Cheng, Chang Li, and Xun Chen. Remote photoplethysmography with an eemd-mcca method robust against spatially uneven illuminations. *IEEE Sensors Journal*, 21(12):13484–13494, 2021.
- [45] Yingli Shi, Jian Qiu, Li Peng, Peng Han, Kaiqing Luo, and Dongmei Liu. A novel non-contact heart rate measurement method based on EEMD combined with FastICA. *Physiol. Meas.*, 44(5), May 2023.
- [46] Xin Liu, Xiaoyu Zhang, Girish Narayanswamy, Yuzhe Zhang, Yuntao Wang, Shwetak Patel, and Daniel McDuff. Deep physiological sensing toolbox. *arXiv preprint arXiv:2210.00716*, 2022.
- [47] Daniel McDuff, Miah Wander, Xin Liu, Brian L. Hill, Javier Hernandez, Jonathan Lester, and Tadas Baltrusaitis. Scamps: Synthetics for camera measurement of physiological signals, 2022.
- [48] Serge Bobbia, Richard Macwan, Yannick Benezeth, Alamin Mansouri, and Julien Dubois. Unsupervised skin tissue segmentation for remote photoplethysmography. *Pattern Recognition Letters*, 124:82–90, 2019. Award Winning Papers from the 23rd International Conference on Pattern Recognition (ICPR).
- [49] Ronny Stricker, Steffen Müller, and Horst-Michael Gross. Non-contact video-based pulse rate measurement on a mobile service robot. In *The 23rd IEEE International Symposium on Robot and Human Interactive Communication*, pages 1056–1062, 2014.
- [50] Xing Zhang, Lijun Yin, Jeffrey F. Cohn, Shaun Canavan, Michael Reale, Andy Horowitz, Peng Liu, and Jeffrey M. Girard. Bp4d-spontaneous: a high-resolution spontaneous 3d dynamic facial expression database. *Image and Vision Computing*, 32(10):692–706, 2014. Best of Automatic Face and Gesture Recognition 2013.
- [51] Rita Meziati Sabour, Yannick Benezeth, Pierre De Oliveira, Julien Chappé, and Fan Yang. Ubfc-phys: A multimodal database for psychophysiological studies of social stress. *IEEE Transactions on Affective Computing*, 14(1):622–636, 2023.
- [52] Jiankai Tang, Kequan Chen, Yuntao Wang, Yuanchun Shi, Shwetak Patel, Daniel McDuff, and Xin Liu. Mmpd: Multi-domain mobile video physiology dataset, 2023.
- [53] Daniel McDuff and Ethan Blackford. iphys: An open non-contact imaging-based physiological measurement toolbox. In *2019 41st annual international conference of the IEEE engineering in medicine and biology society (EMBC)*, pages 6521–6524. IEEE, 2019.
- [54] Guha Balakrishnan, Fredo Durand, and John Guttag. Detecting pulse from head motions in video. In *2013 IEEE Conference on Computer Vision and Pattern Recognition*, pages 3430–3437, 2013.
- [55] Christian Pilz. On the vector space in photoplethysmography imaging. In *Proceedings of the IEEE/CVF international conference on computer vision workshops*, pages 0–0, 2019.
- [56] A functional imaging technique for opto-electronic assessment of skin perfusion. 2008.
- [57] Christian S. Pilz, Jarek Krajewski, and Vladimir Blazek. On the diffusion process for heart rate estimation from face videos under realistic conditions. In Volker Roth and Thomas Vetter, editors, *Pattern Recognition*, pages 361–373, Cham, 2017. Springer International Publishing.
- [58] Christian S. Pilz, Sebastian Zaunseder, Ulrich Canzler, and Jarek Krajewski. Heart rate from face videos under realistic conditions for advanced driver monitoring. *Current Directions in Biomedical Engineering*, 3(2):483–487, 2017.
- [59] Giuseppe Boccignone, Donatello Conte, Vittorio Cuculo, Alessandro D’Amelio, Giuliano Grossi, Raffaella Lanzarotti, and Edoardo Mortara. pyvhr: a python framework for remote photoplethysmography. *PeerJ Computer Science*, 8:e929, 2022.

- [60] Radim Spetlik, Jan Cech, Vojtěch Franc, and Jiri Matas. Visual heart rate estimation with convolutional neural network. 08 2018.
- [61] Mohammad Soleymani, Jeroen Lichtenauer, Thierry Pun, and Maja Pantic. A multimodal database for affect recognition and implicit tagging. *IEEE Transactions on Affective Computing*, 3(1):42–55, 2012.
- [62] Amogh Gudi, Marian Bittner, and Jan van Gemert. Real-time webcam heart-rate and variability estimation with clean ground truth for evaluation. *Applied Sciences*, 10(23), 2020.
- [63] Xuesong Niu, Hu Han, Shiguang Shan, and Xilin Chen. Vipl-hr: A multi-modal database for pulse estimation from less-constrained face video, 2018.
- [64] Constantino Álvarez Casado and Miguel Bordallo López. Face2ppg: An unsupervised pipeline for blood volume pulse extraction from faces, 2023.
- [65] Kegang Wang, Yantao Wei, Mingwen Tong, Jie Gao, Yi Tian, YuJian Ma, and ZhongJin Zhao. Physbench: A benchmark framework for remote physiological sensing with new dataset and baseline. *arXiv preprint arXiv:2305.04161*, 2023.
- [66] Guillaume Heusch, André Anjos, and Sébastien Marcel. A reproducible study on remote heart rate measurement, 2017.
- [67] Dániel Terbe. Camera-based pulse monitoring using deep learning tools. 2021.
- [68] A. Anjos, M. Günther, T. de Freitas Pereira, P. Korshunov, A. Mohammadi, and S. Marcel. Continuously reproducing toolchains in pattern recognition and machine learning experiments. In *International Conference on Machine Learning (ICML)*, August 2017.
- [69] Xiaobai Li, Jie Chen, Guoying Zhao, and Matti Pietikäinen. Remote heart rate measurement from face videos under realistic situations. In *2014 IEEE Conference on Computer Vision and Pattern Recognition*, pages 4264–4271, 2014.
- [70] Sander Koelstra, Christian Muhl, Mohammad Soleymani, Jong-Seok Lee, Ashkan Yazdani, Touradj Ebrahimi, Thierry Pun, Anton Nijholt, and Ioannis Patras. Deap: A database for emotion analysis ;using physiological signals. *IEEE Transactions on Affective Computing*, 3(1):18–31, 2012.
- [71] Justin R. Estep, Ethan B. Blackford, and Christopher M. Meier. Recovering pulse rate during motion artifact with a multi-imager array for non-contact imaging photoplethysmography. In *2014 IEEE International Conference on Systems, Man, and Cybernetics (SMC)*, pages 1462–1469, 2014.
- [72] Zheng Zhang, Jeffrey M. Girard, Yue Wu, Xing Zhang, Peng Liu, Umur Ciftci, Shaun Canavan, Michael Reale, Andrew Horowitz, Huiyuan Yang, Jeffrey F. Cohn, Qiang Ji, and Lijun Yin. Multimodal spontaneous emotion corpus for human behavior analysis. In *2016 IEEE Conference on Computer Vision and Pattern Recognition (CVPR)*, pages 3438–3446, 2016.
- [73] Marco A. F. Pimentel, Alistair E. W. Johnson, Peter H. Charlton, Drew Birrenkott, Peter J. Watkinson, Lionel Tarassenko, and David A. Clifton. Toward a robust estimation of respiratory rate from pulse oximeters. *IEEE Transactions on Biomedical Engineering*, 64(8):1914–1923, 2017.
- [74] Xiaobai Li, Iman Alikhani, Jingang Shi, Tapio Seppänen, Juhani Junttila, Kirsi Majamaa-Voltti, Mikko Tulppo, and Guoying Zhao. The obf database: A large face video database for remote physiological signal measurement and atrial fibrillation detection. In *2018 13th IEEE International Conference on Automatic Face & Gesture Recognition (FG 2018)*, pages 242–249, 2018.
- [75] Ewa Magdalena Nowara, Tim K Marks, Hassan Mansour, and Ashok Veeraraghavan. Sparseppg: Towards driver monitoring using camera-based vital signs estimation in near-infrared. In *Proceedings of the IEEE Conference on Computer Vision and Pattern Recognition Workshops*, page 1272–1281, 2018.
- [76] E. M. Nowara, T. K. Marks, H. Mansour, and A. Veeraraghavan. Near-infrared imaging photoplethysmography during driving. *IEEE Transactions on Intelligent Transportation Systems*, pages 1–12, 2020.
- [77] Mikhail Artemyev, Marina Churikova, Mikhail Grinenko, and Olga S. Perepelkina. Robust algorithm for remote photoplethysmography in realistic conditions. *Digit. Signal Process.*, 104:102737, 2020.
- [78] Rencheng Song, Huan Chen, Juan Cheng, Chang Li, Yu Liu, and Xun Chen. PulseGAN: Learning to generate realistic pulse waveforms in remote photoplethysmography, 2020.
- [79] Zahid Hasan, Sreenivasan Ramasamy Ramamurthy, and Nirmalya Roy. Mpsc-rppg dataset, 2021.
- [80] Taha Samavati, Mahdi Farvardin, and Aboozar Ghaffari. Efficient deep learning-based estimation of the vital signs on smartphones, 2022.



- [81] Hooseok Lee, Hoon Ko, Heewon Chung, Yunyoung Nam, Sangjin Hong, and Jinseok Lee. Real-time realizable mobile imaging photoplethysmography. *Sci. Rep.*, 12(1):7141, May 2022.
- [82] Pieter-Jan Toye. Vital videos: A dataset of videos with ppg and blood pressure ground truths, 2023.
- [83] Macaveiu Gabriela. Mathematical methods in biomedical optics. *International Scholarly Research Notices*, 2013, 2013.
- [84] Lisa Carroll and Tatyana R. Humphreys. Laser-tissue interactions. *Clinics in Dermatology*, 24(1):2–7, 2006.
- [85] Ravimal Bandara. *A Music Keyboard with Gesture Controlled Effects Based on Computer Vision*. PhD thesis, 01 2011.
- [86] John Orazio, Stuart Jarrett, Alexandra Amaro-Ortiz, and Timothy Scott. Uv radiation and the skin. *International Journal of Molecular Sciences*, 14(6):12222–12248, 2013.
- [87] Haiwen Feng, Timo Bolkart, Joachim Tesch, Michael J. Black, and Victoria Abrevaya. Towards racially unbiased skin tone estimation via scene disambiguation, 2022.
- [88] Rakesh Chandra Joshi, Alibert Sánchez Jiménez, and Carlos Manuel Travieso González. Artificial intelligence based multi-sensor covid-19 screening framework. *Tecnología en Marcha*, 35(4):101–109, 2022.
- [89] Xuesong Niu, Shiguang Shan, Hu Han, and Xilin Chen. RhythmNet: End-to-end heart rate estimation from face via spatial-temporal representation. *IEEE Transactions on Image Processing*, 29:2409–2423, 2020.
- [90] Chelsea Finn, Pieter Abbeel, and Sergey Levine. Model-agnostic meta-learning for fast adaptation of deep networks, 2017.

## 7 Appendix

### results

MODEL	TRAIN	TEST	IMG_SIZE	Time_len	MAE	RMSE	MAPE	Pearson
BigSmall	PURE	PURE	72	10	0.68	1.547	0.98	0.981
BigSmall	PURE	PURE	72	20	0.117	0.454	0.163	0.999
BigSmall	PURE	PURE	72	30	0.176	0.556	0.333	0.998
BigSmall	PURE	PURE	72	5	1.598	3.568	2.529	0.914
BigSmall	PURE	UBFC	72	10	3.419	11.862	3.338	0.817
BigSmall	PURE	UBFC	72	20	3.999	13.953	3.533	0.725
BigSmall	PURE	UBFC	72	3	6.285	15.475	6.353	0.711
BigSmall	PURE	UBFC	72	30	5.323	15.329	4.851	0.69
BigSmall	PURE	UBFC	72	5	5.251	14.283	5.156	0.75
BigSmall	UBFC	PURE	72	10	5.819	18.685	5.468	0.636
BigSmall	UBFC	PURE	72	20	4.634	16.923	4.015	0.706
BigSmall	UBFC	PURE	72	3	9.238	19.944	10.24	0.501
BigSmall	UBFC	PURE	72	30	6.071	19.852	5.304	0.573
BigSmall	UBFC	PURE	72	5	7.516	19.226	8.346	0.603
BigSmall	UBFC	PURE	72	10	23.555	35.99	22.892	0.415
BigSmall	UBFC	PURE	72	5	23.547	35.466	24.815	0.33
BigSmall	UBFC	UBFC	72	10	0.586	1.435	0.538	0.994
BigSmall	UBFC	UBFC	72	20	2.539	4.184	2.43	0.947
BigSmall	UBFC	UBFC	72	30	0	0	0	1
BigSmall	UBFC	UBFC	72	5	0.721	2.252	0.712	0.979
BigSmall	UBFC	PURE	72	10	5.718	17.785	5.532	0.677
BigSmall	PURE	UBFC	72	10	3.291	11.376	3.186	0.825
DeepPhys	PURE	PURE	72	10	0.68	1.547	1.079	0.981
DeepPhys	PURE	PURE	72	20	0.117	0.454	0.163	0.999
DeepPhys	PURE	PURE	72	30	0.176	0.556	0.333	0.998
DeepPhys	PURE	PURE	72	5	1.004	2.658	1.511	0.949
DeepPhys	PURE	UBFC	72	10	1.855	7.763	1.904	0.913
DeepPhys	PURE	UBFC	72	20	1.516	5.287	1.557	0.957
DeepPhys	PURE	UBFC	72	3	4.646	12.756	4.812	0.778
DeepPhys	PURE	UBFC	72	30	1.684	5.988	1.745	0.949

DeepPhys	PURE	UBFC	72	5	2.609	9.021	2.647	0.884
DeepPhys	UBFC	PURE	72	10	5.635	17.641	6.076	0.674
DeepPhys	UBFC	PURE	72	20	4.896	17.153	4.673	0.701
DeepPhys	UBFC	PURE	72	3	7.857	17.698	9.472	0.627
DeepPhys	UBFC	PURE	72	30	3.662	13.585	3.588	0.819
DeepPhys	UBFC	PURE	72	5	7.111	17.926	8.497	0.663
DeepPhys	UBFC	PURE	72	10	26.719	39.369	26.05	0.178
DeepPhys	UBFC	PURE	72	20	25.195	39.839	22.811	0.019
DeepPhys	UBFC	PURE	72	5	23.027	33.922	24.852	0.392
DeepPhys	UBFC	UBFC	72	10	0.977	2.748	1.069	0.975
DeepPhys	UBFC	UBFC	72	20	2.148	3.262	2.04	0.965
DeepPhys	UBFC	UBFC	72	30	3.809	9.329	3.283	0.537
DeepPhys	UBFC	UBFC	72	5	0.721	2.252	0.722	0.981
DeepPhys	UBFC	UBFC	72	10	0.879	1.758	0.893	1
DeepPhys	UBFC	UBFC	72	20	0	0	0	1
DeepPhys	UBFC	UBFC	72	30	0	0	0	1
DeepPhys	UBFC	UBFC	72	5	4.688	11.951	4.663	0.775
EfficientPhys	PURE	PURE	72	10	0.567	1.412	0.94	0.991
EfficientPhys	PURE	PURE	72	20	0	0	0	1
EfficientPhys	PURE	PURE	72	30	0.176	0.556	0.333	0.999
EfficientPhys	PURE	PURE	72	5	0.974	2.616	1.474	0.969
EfficientPhys	PURE	UBFC	72	10	1.278	6.402	1.313	0.938
EfficientPhys	PURE	UBFC	72	20	1.376	5.991	1.373	0.942
EfficientPhys	PURE	UBFC	72	3	4.344	12.343	4.412	0.792
EfficientPhys	PURE	UBFC	72	30	1.43	5.837	1.395	0.942
EfficientPhys	PURE	UBFC	72	5	2.208	8.455	2.197	0.892
EfficientPhys	UBFC	PURE	72	10	3.33	12.931	3.543	0.834
EfficientPhys	UBFC	PURE	72	20	2.49	11.287	2.514	0.873
EfficientPhys	UBFC	PURE	72	3	8.358	18.714	10.177	0.566
EfficientPhys	UBFC	PURE	72	30	1.743	8.45	2.02	0.93
EfficientPhys	UBFC	PURE	72	5	5.794	15.515	7.061	0.748
EfficientPhys	UBFC	PURE	72	10	13.887	23.307	14.522	0.746
EfficientPhys	UBFC	PURE	72	20	15.625	28.416	14.746	0.633
EfficientPhys	UBFC	PURE	72	5	15.044	26.045	15.182	0.668
EfficientPhys	UBFC	UBFC	72	10	0.586	2.269	0.675	0.979
EfficientPhys	UBFC	UBFC	72	20	2.197	3.479	2.035	0.95
EfficientPhys	UBFC	UBFC	72	30	3.516	8.292	3.048	0.536
EfficientPhys	UBFC	UBFC	72	5	0.27	1.379	0.268	0.99
TSCAN	PURE	PURE	72	10	0.68	1.547	1.079	0.981
TSCAN	PURE	PURE	72	20	0.117	0.454	0.163	0.999
TSCAN	PURE	PURE	72	30	0.176	0.556	0.333	0.998
TSCAN	PURE	PURE	72	5	0.959	2.596	1.48	0.954
TSCAN	PURE	UBFC	72	10	2.296	9.068	2.315	0.884
TSCAN	PURE	UBFC	72	20	1.435	5.3	1.44	0.956
TSCAN	PURE	UBFC	72	3	4.424	12.432	4.623	0.796
TSCAN	PURE	UBFC	72	30	1.634	6.089	1.488	0.942
TSCAN	PURE	UBFC	72	5	2.388	8.85	2.467	0.89
TSCAN	UBFC	PURE	72	10	3	12.098	3.286	0.859
TSCAN	UBFC	PURE	72	20	3.249	12.525	3.265	0.846
TSCAN	UBFC	PURE	72	3	8.232	18.453	9.62	0.588
TSCAN	UBFC	PURE	72	30	1.628	7.435	1.924	0.948
TSCAN	UBFC	PURE	72	5	5.093	14.907	6.069	0.777
TSCAN	UBFC	PURE	72	10	24.609	37.156	24.768	0.366
TSCAN	UBFC	PURE	72	20	24.805	38.792	21.923	0.417
TSCAN	UBFC	PURE	72	5	22.075	34.563	22.586	0.364
TSCAN	UBFC	UBFC	72	10	1.367	3.612	1.48	0.955

Remote Bio-Sensing : Open Source Benchmark Framework for Fair Evaluation of rPPG

TSCAN	UBFC	UBFC	72	20	2.148	3.262	2.04	0.965
TSCAN	UBFC	UBFC	72	30	4.688	9.574	4.064	0.513
TSCAN	UBFC	UBFC	72	5	0.361	1.592	0.368	0.989
TSCAN	UBFC	UBFC	72	10	0	0	0	1
TSCAN	UBFC	UBFC	72	20	0	0	0	1
TSCAN	UBFC	UBFC	72	5	4.922	13.525	4.911	0.763

Table 5: fit.yaml

```

model_save_path: "" # model save path
preprocess:
  flag: true # true: preprocess, false: not preprocess
wandb:
  flag: false
  project_name: DeepPhys
  entity: wandb_entity

fit:
  model: DeepPhys # model name
  type: DIFF # model type ( DIFF, CONT )
  time_length: 180 # model's target length
  overlap_interval: 0 # default 0
  img_size: 72 # model's input size
  train_flag: True
  eval_flag: True
  eval_interval: 100 # force evaluation step
  debug_flag: False # True: debug mode, False: train mode

train:
  dataset: UBFC
  shuffle: True
  fs: 30 # video fps
  batch_size: 4 # batch size
  learning_rate: 0.009 # learning rate
  epochs: 30 # epochs
  loss: MSE # loss function
  optimizer: AdamW # optimizer
  meta: # meta Learning Configuration for MAML
    flag: false
    inner_optim: adam
    inner_loss: MSE
    inner_lr: 0.01

test:
  dataset: PURE
  shuffle: False
  fs: 30
  batch_size: 4
  cal_type: FFT # Heart rate calculation method
  metric: [ 'MAE', 'RMSE', 'MAPE', 'Pearson' ]
  eval_time_length: 10 # second

```